Relationship between computed tomography and histological features of gastrointestinal stromal tumors

Nesrin Gunduz, Mahmut Bilal Dogan, Hatice Seneldir¹, Ozgur Ekinci², Ihsan Metin Leblebici², Orhan Alimoglu²

Departments of Radiology, ¹Pathology and ²General Surgery, Faculty of Medicine, Goztepe Prof. Dr. Suleyman Yalcin City Hospital, Istanbul Medeniyet University, Istanbul, Turkey

Abstract

Background and Aim: Histomorphological and immunohistochemical (IHC) properties of gastrointestinal stromal tumors (GISTs) allow for accurate diagnosis and determine the prognosis. We aimed to evaluate the relationship between the computed tomography (CT) features, histomorphological properties, and IHC markers.

Materials and Methods: This retrospective study comprised patients with pathologically confirmed GISTs between 2016 and 2021. The predefined CT characteristics comprised tumor size, hemorrhage and calcification, CT-growth pattern (exophytic/endophytic), and contrast enhancement pattern of the solid component (homogeneous/heterogeneous). The GISTs were divided into groups according to the National Institutes of Health risk category, cell type, presence of necrosis, CD117 and α -SMA positivity, and Ki-67 index. The frequencies of CT phenotypes were compared between groups.

Results: Overall 24 (14 [58.3%] males) patients with a median age of 64 (59.5–75.5) having 25 GISTs were included. Of 25 GISTs, 16 (64%) were gastric and 9 (36%) were intestinal in origin. Among CT features, the maximum diameter was higher in epithelioid, infiltrative, a mitotic count ≥5/50, necrotic, high-risk GISTs (P < 0.05 for all). The median tumor size was higher in Ki-67 >8 than Ki-67 <6 subjects (112.5 [39.25–153.75] vs. 22.5 [16.75–57.5] mm, P = 0.014). A heterogeneous enhancement was also more frequent in Ki-67 >8 tumors (P = 0.04). The enhancement pattern did not differ according to CD-117 or SMA positivity. Logistic regression analysis revealed that the only independent predictor of a Ki-67 >8 status was the tumor size (odds ratio: 1.02, 95% confidence interval: 1.001–1.046, P = 0.04).

Conclusions: Heterogeneously enhanced large GISTs at CT imaging strongly suggest the presence of poor prognostic factors including a high Ki-67 index and/or high-risk category.

Keywords: Computed tomography, gastrointestinal stromal tumor, Ki 67 index

Address for correspondence: Dr. Mahmut Bilal Dogan, No: 161/1, Kadikoy, Egitim, Istanbul 34722, Turkey.

E-mail: mahmutbilaldogan@gmail.com

Submitted: 22-Aug-2023 Revised: 16-Jan-2024 Accepted: 13-Feb-2024 Published: 22-May-2024

INTRODUCTION

Gastrointestinal stromal tumors (GISTs) originate from the interstitial cells of Cajal and are the most common mesenchymal tumors arising from the gastrointestinal

Access this article online					
Quick Response Code:	Website:				
	https://journals.lww.com/wajr				
	DOI: 10.4103/wajr.wajr_19_23				

tract.^[1] The most common site of origin is the stomach followed by the small intestine.^[2] The definitive diagnosis of GIST is based on histomorphology and immunohistochemical (IHC) techniques including

This is an open access journal, and articles are distributed under the terms of the Creative Commons Attribution-NonCommercial-ShareAlike 4.0 License, which allows others to remix, tweak, and build upon the work non-commercially, as long as appropriate credit is given and the new creations are licensed under the identical terms.

 $\textbf{For reprints contact:} \ WKHLRPMedknow_reprints@wolterskluwer.com$

How to cite this article: Gunduz N, Dogan MB, Seneldir H, Ekinci O, Leblebici IM, Alimoglu O. Relationship between computed tomography and histological features of gastrointestinal stromal tumors. West Afr J Radiol 2023;30:1-7.

positive staining mainly with CD117 and Delay of Germination-1 (DOG1).^[3] Desmin and S-100 are rarely detected in GISTs, and the α-SMA may show positive staining in a considerable number of cases.^[4] Surgical resection is the treatment of choice for cure when feasible. In instances where patients cannot undergo surgery or there is recurrence, targeted therapy with tyrosine kinase inhibitor imatinib may be required. The recurrence of GISTs can be predicted by mitotic count, tumor size, and tumor site based on the National Institute of Health (NIH) criteria.^[5] More recently, human nuclear cell proliferation-associated antigen Ki-67 was proposed as a prognostic predictor in GISTs.^[6,7]

Contrast-enhanced computed tomography (CT) is the standard radiologic technique for imaging GISTs.[8] CT is very useful for the assessment of tumor size, CT-growth pattern (exo/endophytic enlargement), contrast enhancement, presence of intratumoral cystic changes, hemorrhage, calcification, lymphatic involvement, and distant metastasis. Documented evidence is available regarding the relationship between several CT and histomorphological properties in patients with GISTs. [2,9,10] One study has also found a relationship between CT findings and a prognostic IHC marker, Ki-67.[7] However, no study has evaluated the relationship between CT characteristics and the status of diagnostic IHC markers in patients with GISTs. Recognition of these differences by CT may be important for the precision of diagnosis and prognosis in those who are not eligible for surgery or whose surgery will be deferred for a period of time.

In the current study, we aimed to evaluate the relationship between the CT features and diagnostic IHC marker positivity in addition to histomorphological properties and Ki-67 staining status.

MATERIALS AND METHODS

This single-center retrospective study comprised patients with pathologically confirmed GIST in our tertiary referral center between 2016 and 2021. The criteria for inclusion comprised a preoperative dynamic-enhanced CT imaging, surgical resection to be performed in our institute, and a comprehensive histomorphological and IHC assessment of the tumor. The exclusion criteria were inadequate image quality and absence of IHC analysis.

Contrast-enhanced dynamic CT was performed in all cases before surgery. The images were reloaded from the picture archiving and communication system of our institute. CT images were reviewed by two readers including one 10-year experienced radiologist in abdominal cross-sectional

imaging and one radiology resident who has completed the abdominal radiology training. Both readers were blinded to the histopathological data. Institutional ethics committee approval was obtained. Patients' age and gender, CT features, and histomorphological and IHC properties were recorded in a database.

The macroscopic analysis of the gross tumor included the origin (gastric or intestinal) and the growth pattern (infiltrative or expansive). The microscopic sections were evaluated in terms of cell morphology (spindled or epithelioid), cytoplasmic staining pattern with hematoxylin and eosin, nucleus morphology, and mitotic activity. Since most GISTs have a mutation of c-KIT proto-oncogene, [11] CD117 positivity was used for IHC diagnosis. For those with CD117-negative GISTs, DOG1 (discovered on GIST-1) positivity was used for exact diagnosis. [12]

The scanner was a 128-slice MDCT (GE Healthcare Optima CT660, USA). The scanning protocol included precontrast and contrast-enhanced portal phase (1.5 mL/kg of iopromide [Ultravist 370; Schering, Berlin, Germany]) images in all patients. After the start of dye injection using the bolus tracking technique, the portal venous phase at the 60th s was obtained. Postprocessing techniques included axial, oblique, coronal, and curved multi-planar reformatting, maximum and minimum intensity of projections. The images were reconstructed with a slice thickness of 2.5-3.0 mm and a reconstruction interval of 1.5-2 mm. The predefined CT characteristics comprised tumor size, presence of intratumoral cystic openings, hemorrhage and calcification, CT-growth pattern (exophytic/endophytic), CT attenuation of the solid component (hypo-isodense/ hyperdense), and contrast enhancement pattern of the solid component (homogeneous/heterogeneous).

Statistical analysis was performed with SPSS 26.0 (IBM SPSS Inc., Chicago, IL, USA). The normality of continuous variables was analyzed by the Shapiro–Wilk test. Descriptive statistics were reported as median with 25th–75th percentiles since the data distribution was not normal. Categorical variables were reported as frequencies with percentages.

The patients were divided into groups according to the NIH risk category. ^[1] For the purpose of the present study, the GISTs with intermediate- or high-risk categories were merged as group high risk, whereas those with very low or low risk were merged as group low risk. Moreover, additional categorizations were formed according to histomorphological and IHC features. The atypical IHC expression pattern was considered whenever one of the following three patterns was present a GIST with no

expression of either CD117 or DOG1, a negative CD34 despite positivity of CD117 and DOG1 in those with gastric spindled cell GIST, and a positivity for S-100 or desmin despite confirmed GIST with CD117 and DOG1 positivity.

The frequencies of CT phenotypes were compared between groups. Independent two-group comparisons for continuous variables were tested using the Mann–Whitney U-test. The proportions were compared between the groups using Pearson's Chi-square test in case the assumptions were met. Otherwise, Fisher's exact test was used. For predicting the Ki-67 status, a multivariate analysis was performed using logistic regression and odds ratios (ORs) with 95% confidence intervals (CI) were provided. Inter-reader agreement for categorical variables was assessed by kappa statistics. Continuous variables were analyzed by intraclass correlation coefficient in terms of interobserver agreement. The significance level was accepted at P < 0.05 for all statistical analyses.

RESULTS

In total, 24 patients, comprising 14 males (58.3%) and 10 females (41.7%), with a median age of 64 (range: 59.5–75.5), were enrolled, and they collectively presented with 25 GISTs. All patients had single tumors except for one patient who had two distinct gastric GISTs which were separately included in the statistical analyses. Of 25 GISTs, 16 (64%) originated from the gastric wall and 9 (36%) from the small intestinal wall. Distant metastasis was found in 3 cases (2 gastric GIST and 1 intestinal GIST). Lymphatic involvement was not present in any case.

Macroscopic growth pattern was expansive in 21 (84%) and infiltrative in 4 (16%) GISTs. The predominant cell type was spindled in 20 (80%), epithelioid in 1 (4%), and mixed in 4 (16%) tumors. Due to a low number of cases, the epithelioid and mixed types were merged and compared with the pure spindle cell type in terms of CT features. The mitotic rate was <5/50 in 19 (76%) and $\ge 5/50$ in 6 (24%) cases. Histologically confirmed necrosis was present in 7 (28%) GISTs. The tumor grade was high in 7 (28%) and low in 18 (72%) masses. The frequencies of T stages of GISTs from T1 to T4 were 5 (20%), 6 (24%), 4 (16%), and 10 (40%), respectively. IHC staining revealed CD-117 positivity in 21 (86%), DOG-1 positivity in 23 (92%), CD-34 positivity in 23 (92%), and SMA positivity in 8 (32%) subjects. Desmin and S-100 remained negative in most cases, except for only 2 and 1 cases with positive staining, respectively. A proliferation index of Ki-67 < 6 was present in 15 (60%) and Ki-67 > 8 in 10 (40%) GISTs. No case with a Ki-67 index between 6 and 8 was observed. The modified NIH risk category of GISTs was low in 13 cases and high in 12 cases.

The median tumor size was 75.2 (22–117.5) mm measured from the maximum diameter. The CT-growth pattern was exophytic in 18 (72%) and endophytic in 7 (18%). Cystic openings were present in 8 (32%), hemorrhage in 4 (16%), and calcification in 1 (4%) GIST. The tumors were hypodense in 9 (36%), isodense in 4 (16%), and hyperdense in 12 (48%) cases. The enhancement pattern was heterogeneous in 16 (64%) and homogeneous in 9 (36%) tumors.

The GISTs were grouped according to the histomorphological features including tumor origin, cell type, growth pattern, mitotic count, presence of necrosis, and NIH risk category.

The maximum diameter measured at CT differed significantly between the dichotomized subgroups for all histomorphological subsets [P < 0.05 for all comparisons, Table 1] except for the tumor origin.

The frequency of intratumoral cystic changes as assessed by CT was not related to histomorphological subgroups except for cell type. The intratumoral cystic changes were more common in epithelioid GISTs than spindled tumors (4 [80%] vs. 4 [20%], respectively, P = 0.023).

The rate of heterogeneous enhancement by CT was higher in histologically necrotic (7 [100%]) GISTs than nonnecrotic (9 [50%]) tumors (P = 0.027). A heterogeneous enhancement was also more common in high-risk tumors (12 [85.7%]) than low-risk (4 [36.4%]) GISTs.

The remaining CT features (intratumoral bleeding, CT-growth pattern, and CT attenuation of solid component) were not associated with any other histomorphological feature. The details of intergroup CT differences are demonstrated in Table 1.

The GISTs were grouped according to the status of IHC staining with CD-117, α -SMA, and Ki-67 separately. Because the numbers of cases with positive desmin (n = 2) and S-100 (n = 1) and negative DOG-1 (n = 1) were very low, the GISTs were not categorized as per these markers separately. In addition to individual staining status for each IHC marker, GISTs were classified to have typical or atypical IHC staining pattern. A total of 8 GISTs were considered to have atypical IHC staining 17 cases were considered to have a typical IHC expression pattern.

The median tumor size was higher in Ki-67 >8 cases than Ki-67 <6 subjects (112.5 [39.25–153.75] vs. 22.5 [16.75–57.5] mm, respectively, P = 0.014). No relationship was found between size and CD-117 or SMA [Table 2]. The median tumor size was similar between typical (53 [32–111]) and atypical (50.5 [19.5–145.5]) IHC staining subgroups (P = 0.977).

A heterogeneous CT enhancement was more frequent in Ki-67 >8 versus Ki-67 <6 tumors (90% vs. 46.7%, respectively, P = 0.04) [Figures 1 and 2]. The enhancement pattern did not differ according to CD-117 or SMA positivity. The enhancement pattern was also similar between typical and atypical IHC staining patterns [Figure 3]. A logistic regression model including heterogeneous enhancement and tumor size as covariates to predict Ki-67 status was

constructed. The only independent predictor of a Ki-67 >8 status was the tumor size (OR: 1.02, 95% CI: 1.001–1.046, P=0.04), whereas heterogeneous enhancement (OR: 2.88, 95% CI: 0.213–38.882, P=0.426) was insignificant in the model.

A relationship between the remaining CT features (intratumoral cystic changes, intratumoral bleeding, CT-growth pattern, and CT attenuation) and individual IHC markers was not found. The CT features according to the IHC staining status are demonstrated in detail in Table 2.

Interobserver agreement for enhancement pattern (kappa = 0.67, P = 0.01) and presence of cystic changes (kappa = 0.72, P < 0.001) at CT imaging were

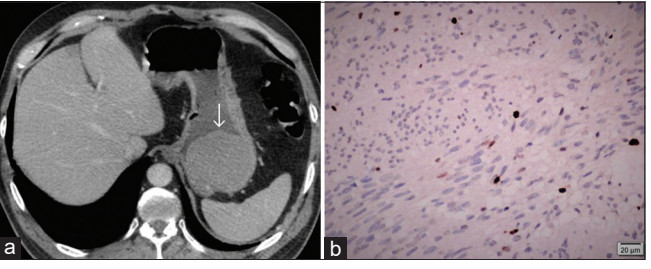


Figure 1: A 50-year-old man with a gastrointestinal stromal tumor in the stomach. (a) Axial contrast-enhanced computed tomography showing a well-defined soft-tissue mass with homogeneous enhancement in the stomach (arrow). (b) In tumor cells, expression of Ki-67 is observed at a rate of 2% (×400)

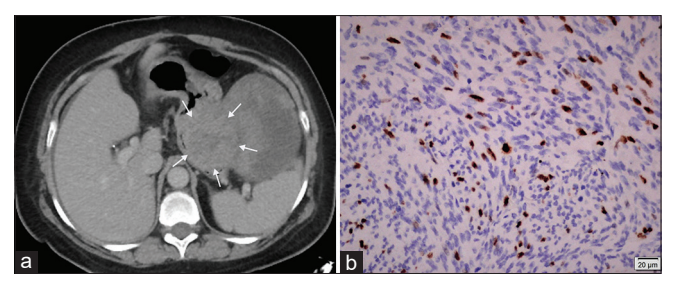


Figure 2: An 87-year-old woman with gastrointestinal stromal tumor in the stomach. (a) Coronal contrast-enhanced computed tomography showing a well-defined, large soft-tissue mass with heterogeneous enhancement in the stomach (arrow). (b) In tumor cells, expression of Ki-67 is observed at a rate of 15% (×400)

Table 1: Comparison of computed tomography features according to histomorphological phenotypes

Histomorphological subsets	CT features							
	Size, median (IQR) (mm)	Cystic changes, n (%)	Bleeding, n (%)	Exophytic CT-growth pattern, n (%)	Hyperdensity, n (%)	Heterogeneous enhancement, n (%)		
Origin	P=0.213	P=0.182	<i>P</i> =0.602	P=0.673	P=0.226	<i>P</i> =0.671		
Gastric (n=16)	53 (37-117)	7 (43.8)	2 (12.5)	12 (75)	6 (37.5)	11 (68.8)		
Intestinal (n=9)	32 (21-114)	1 (11.1)	2 (22.2)	6 (66.7)	6 (66.7)	5 (55.6)		
Growth	P=0.012	P=0.57	P=0.527	P=0.294	P=0.593	P=0.26		
Expansive $(n=21)$	37.5 (21-87.5)	6 (28.6)	3 (14.3)	14 (66.7)	11 (52.4)	12 (57.1)		
Infiltrative (n=5)	143 (116-228.5)	2 (50)	1 (25)	4 (100)	1 (25)	4 (100)		
Cell type*	P=0.035	P=0.023	P=1	P=0.274	P=0.322	P=0.123		
Spindled (n=20)	41 (22-87.5)	4 (20)	3 (15)	13 (65)	11 (55)	11 (55)		
Epithelioid (n=5)	165 (121 – 177)	4 (80)	1 (20)	5 (100)	1 (20)	5 (100)		
Mitotic count	P=0.012	P=1	P=0.234	P=0.637	P=0.16	P=0.364		
<5/50 (n=19)	33.5 (21-71)	6 (31.6)	2 (10.5)	13 (68.4)	11 (57.9)	11 (57.9)		
$\geq 5/50 \ (n=6)$	132 (104-165)	2 (33.3)	2 (33.3)	5 (83.3)	1 (16.7)	5 (83.3)		
Necrosis	P=0.034	P=0.64	P=0.548	P=0.133	P=0.073	P=0.027		
Absent (n=18)	34 (21-53)	5 (27.8)	2 (11.1)	11 (61.1)	11 (61.1)	9 (50)		
Present (n=7)	114 (107.5 - 143)	3 (42.9)	2 (28.6)	7 (100)	1 (14.3)	7 (100)		
Risk category	<i>P</i> <0.001	P= 1	P=0.105	P=0.177	<i>P</i> =0.378	P=0.017		
Low (n=13)	21 (15.5-32.5)	3 (27.3)	0	6 (54.5)	7 (63.6)	4 (36.4)		
High $(n=12)$	112.5 (60–150)	5 (35.7)	4 (28.6)	12 (85.7)	5 (35.7)	12 (85.7)		

^{*}Due to the low number of cases, only one epithelioid GIST was merged with four mixed GISTs. The first column of this crosstable includes the categorization of study patients according to the microscopically assessed histomorphological subsets. Each subset includes dichotomization of the study group (i.e., gastric or intestinal, expansive or infiltrative, etc.). The frequencies of CT features for each dichotomized subset are given in the corresponding cells contained in the row of that subset. Of note, only the size is a continuous variable and hence it is reported as median diameter with IQR, rather than frequency. The *P* values provided in each cell show the statistical result of the comparison of the frequency of CT features between the dichotomized groups of every subset. CT — Computed tomography, IQR — Interquartile range, GIST — Gastrointestinal stromal tumor

Table 2: Comparison of computed tomography features according to immunohistochemical phenotypes

Immunohistochemical CT features

Immunohistochemical subsets	CT features						
	Size, median (IQR) (mm)	Cystic changes, n (%)	Bleeding, n (%)	Exophytic CT-growth pattern, n (%)	Hyperdensity, n (%)	Heterogeneous enhancement, n (%)	
CD-117	P=0.604	<i>P</i> =1	<i>P</i> =0.106	<i>P</i> =1	<i>P</i> =1	P=0.602	
Negative (n=4)	114 (60.5-115.5)	1 (25)	2 (50)	3 (75)	2 (50)	2 (50)	
Positive (n=21)	41 (23-111)	7 (33.3)	2 (9.5)	15 (71.4)	10 (47.6)	14 (66.7)	
SMA	P=0.153	P= 1	P=1	P=0.64	P=1	<i>P</i> =0.411	
Positive (n=8)	27.5 (15.5-107)	2 (25)	1 (12.5)	5 (62.5)	5 (62.5)	5 (62.5)	
Negative (n=17)	50 (32.5-135.5)	6 (35.3)	3 (17.6)	13 (76.5)	11 (64.7)	7 (41.2)	
IHC staining	<i>P</i> =0.977	<i>P</i> =1	<i>P</i> =0.57	<i>P</i> =0.64	<i>P</i> =1	P=0.39	
Atypical (n=8)	50 (19.5-145.5)	3 (37.5)	2 (25)	3 (37.5)	4 (50)	4 (50)	
Typical (n=17)	53 (32-111)	5 (29.4)	2 (11.8)	4 (23.5)	8 (47.1)	12 (70.6)	
Ki-67	P=0.014	P=0.667	<i>P</i> =0.267	P=0.179	<i>P</i> =0.688	<i>P</i> =0.04	
>8 (<i>n</i> =10)	112.5 (41-150)	4 (40)	3 (30)	9 (90)	4 (40)	9 (90)	
<6 (n=15)	27.5 (18-53)	4 (26.7)	1 (6.7)	9 (60)	8 (53.3)	7 (46.7)	

The first column of this crosstable includes the categorization of study patients according to the immunohistochemical subsets. Each subset includes dichotomization of the study group (i.e., CD-117 negative or positive, SMA positive or negative, etc.). The frequencies of CT features for each dichotomized subset are given in the corresponding cells contained in the row of that subset. Of note, only the size is a continuous variable and hence it is reported as median diameter with IQR, rather than frequency. The *P* values provided in each cell show the statistical result of the comparison of the frequency of CT features between the dichotomized groups of every subset. CT – Computed tomography, IQR – Interquartile range, IHC – Immunohistochemical, SMA – Smooth muscle actin, CD – Cluster of differentiation

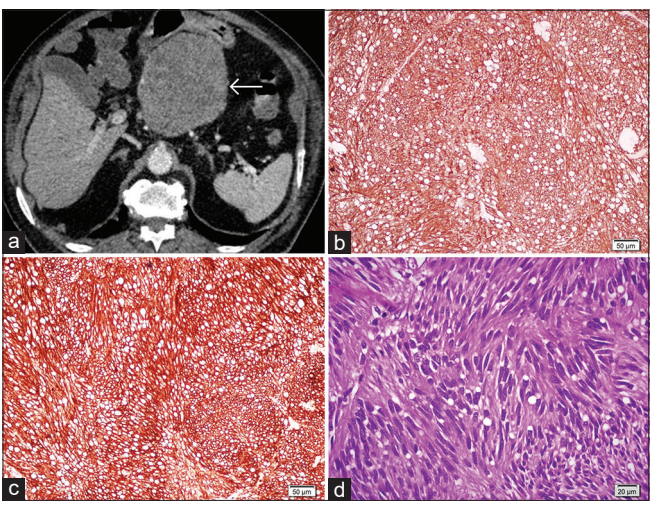


Figure 3: A 79-year-old man with a gastrointestinal stromal tumor in the stomach. (a) Axial contrast-enhanced computed tomography showing a well-defined, soft-tissue mass in the stomach (arrow). The mass does not contain cystic components. (b) CD117 expression in tumor cells (×200). (c) Delay of Germination-1 expression in tumor cells (×200). (d) Spindle-shaped cells and paranuclear vacuoles forming the tumor (H and E, ×400)

substantial. A near-perfect agreement (intraclass correlation coefficient = 0.93, 95% CI: 0.86-0.97, P < 0.001) was observed for size assessment between the readers.

DISCUSSION

This study evaluated four main issues including the comparison of CT features between high- and low-risk GISTs based on NIH consensus criteria, the comparison of CT features according to the individual components (mitotic count, tumor size, and tumor site) of NIH consensus criteria, the comparison of CT features as per other relevant histomorphological properties, and the comparison of CT

features as per staining status with relevant diagnostic and prognostic IHC markers.

The principal findings were a larger size and heterogeneous enhancement at CT were more frequent in high NIH risk category GISTs, an elevated mitotic count was correlated with a greater size in GISTs, whereas the tumor site did not exhibit an association with size or CT phenotype. The tumor size was larger in epithelioid GISTs, infiltrative GISTs, and GISTs with necrosis, and a high Ki-67 index was associated with larger size and heterogeneous enhancement at CT imaging. CD117 or α-SMA positivity or atypical IHC staining pattern did not affect the CT phenotype.

The high frequency of heterogeneous enhancement pattern in patients with high NIH risk category or Ki-67 >8 status indicates a relationship between prognosis and contrast enhancement patterns of GISTs. Similarly, Ulusan *et al.* found a relationship between heterogeneous enhancement and a high mitotic index, a marker of poor prognosis. [11] On the other hand heterogeneous enhancement did not independently predict a Ki-67 >8 status when adjusted for tumor size in the current study. This finding supports the previous observations of a more homogeneous enhancement with small GISTs and mostly heterogeneous enhancement with large tumors. [12,13]

The macroscopic tumor size is widely recognized as a major determinant of malignant behavior of GISTs.^[14] A larger tumor has been reported to be associated with a more aggressive course, increased recurrence risk, and reduced survival.^[15] In the current study, the CT tumor size was consistently different between all histomorphological

subtypes except for tumor origin. The GIST was larger in infiltrative GISTs than expansive GISTs. Epithelioid GISTs were larger as compared to spindled cell tumors. The GISTs with high mitotic count were larger than those with the low mitotic count. The GISTs with necrosis were larger than those without necrosis. A larger tumor was observed in high-risk GIST as compared to low-risk GIST, which can be attributed to tumor size and mitotic count which are already the components of risk categorization. Interestingly, the tumor size was similar between intestinal and gastric GISTs despite the previous observations of a worse prognosis with intestinal origin. [16,17] Moreover, the origin of the tumor was not associated with any CT feature in our series.

The mitotic count, which reflects the cellularity of a GIST, has been reported as a major predictor of prognosis. [17,18] The CT attenuation of GISTs has been shown to be lower than non-GIST benign subepithelial tumors, although the underlying mechanism was unclear. [19] One would expect a difference in the CT density of solid components of GISTs between hyper versus hypocellular tumors. However, the CT density was similar between high and low mitotic count GISTs in our study. Moreover, no other CT feature differed significantly between the high and low mitotic count subgroups. This result was consistent with previous studies demonstrating no relationship between most CT features and mitotic count. [9,20] In addition, the Ki-67 index, a robust marker of proliferation, was also not related to the attenuation pattern of GISTs in our work. On the other hand, Li et al. have found a moderate (r = 0.619) correlation between mitotic count and Ki-67 index. [7] However, the cutoff values used in Li et al. study were not identical to the thresholds used in the current study. We argue that the CT density of GIST does not necessarily depend on the cellularity or prognostic risk. In addition to cellularity, the water content and intratumoral hemorrhage are the potential confounders affecting the CT density of GISTs.

An exophytic CT-growth pattern of GISTs at CT imaging has been linked to higher risk as compared to endophytic pattern in one study. [21,22] A mixed growth pattern at CT was reported as an independent predictor of risk in another work. [23] In the current study, a trend toward a higher frequency of exophytic pattern in high-risk GIST was observed. Larger and prospective studies are required to clarify the relationship between the prognosis and an exophytic GIST at preoperative CT.

The study has some limitations. The study relies on retrospective data, which may be subject to selection bias and limitations inherent in retrospective analyses. The study's sample size is relatively small, which could affect the statistical power and the ability to detect subtle associations.

CONCLUSIONS

Heterogeneously enhanced large GISTs at CT imaging strongly suggest the presence of poor prognostic factors including a high Ki-67 index and/or high-risk category. CT features of GISTs do not appear to be associated with diagnostic IHC staining status except for Ki-67.

Acknowledgments

The abstract of the article was accepted as a "Research Presentation" at the 32nd ESGAR (European Society of Gastrointestinal and Abdominal Radiology) Annual Meeting, 2021.

Financial support and sponsorship

Nil.

Conflicts of interest

There are no conflicts of interest.

REFERENCES

- Joensuu H, Hohenberger P, Corless CL. Gastrointestinal stromal tumour. Lancet 2013;382:973-83.
- Baheti AD, Shinagare AB, O'Neill AC, Krajewski KM, Hornick JL, George S, et al. MDCT and clinicopathological features of small bowel gastrointestinal stromal tumours in 102 patients: A single institute experience. Br J Radiol 2015;88:20150085.
- Schaefer IM, Mariño Enríquez A, Fletcher JA. What is new in gastrointestinal stromal tumor? Adv Anat Pathol 2017;24:259-67.
- Hirota S. Differential diagnosis of gastrointestinal stromal tumor by histopathology and immunohistochemistry. Transl Gastroenterol Hepatol 2018;3:27.
- Lanke G, Lee JH. How best to manage gastrointestinal stromal tumor. World J Clin Oncol 2017;8:135-44.
- Zhang H, Liu Q. Prognostic indicators for gastrointestinal stromal tumors: A review. Transl Oncol 2020;13:100812.
- Li H, Ren G, Cai R, Chen J, Wu X, Zhao J. A correlation research of Ki67 index, CT features, and risk stratification in gastrointestinal stromal tumor. Cancer Med 2018;7:4467-74.
- Sandrasegaran K, Rajesh A, Rushing DA, Rydberg J, Akisik FM, Henley JD. Gastrointestinal stromal tumors: CT and MRI findings. Eur Radiol 2005;15:1407-14.
- Iannicelli E, Carbonetti F, Federici GF, Martini I, Caterino S, Pilozzi E, et al. Evaluation of the relationships between computed tomography features, pathological findings, and prognostic risk assessment in gastrointestinal stromal tumors. J Comput Assist Tomogr 2017;41:271-8.
- Levy AD, Remotti HE, Thompson WM, Sobin LH, Miettinen M. Gastrointestinal stromal tumors: Radiologic features with pathologic correlation. Radiographics 2003;23:283-304, 456.
- Ulusan S, Koc Z, Kayaselcuk F. Gastrointestinal stromal tumours: CT findings. Br J Radiol 2008;81:618-23.
- Ghanem N, Altehoefer C, Furtwängler A, Winterer J, Schäfer O, Springer O, et al. Computed tomography in gastrointestinal stromal tumors. Eur Radiol 2003;13:1669-78.
- Yu MH, Lee JM, Baek JH, Han JK, Choi BI. MRI features of gastrointestinal stromal tumors. AJR Am J Roentgenol 2014;203:980-91.

Gunduz, et al.: CT and histological features of GIST

- Maldonado FJ, Sheedy SP, Iyer VR, Hansel SL, Bruining DH, McCollough CH, et al. Reproducible imaging features of biologically aggressive gastrointestinal stromal tumors of the small bowel. Abdom Radiol (NY) 2018;43:1567-74.
- Joensuu H, Vehtari A, Riihimäki J, Nishida T, Steigen SE, Brabec P, et al. Risk of recurrence of gastrointestinal stromal tumour after surgery: An analysis of pooled population-based cohorts. Lancet Oncol 2012;13:265-74.
- Ekinci O, Leblebici M, Acar M, Erol CI, Alimoglu O. Risk Factors of Gastrointestinal Stromal Tumor Recurrence. Anatolian Clin 2021;26:3-10.
- Burkill GJ, Badran M, Al Muderis O, Meirion Thomas J, Judson IR, Fisher C, et al. Malignant gastrointestinal stromal tumor: Distribution, imaging features, and pattern of metastatic spread. Radiology 2003;226:527-32.
- Demetri GD, von Mehren M, Antonescu CR, DeMatteo RP, Ganjoo KN, Maki RG, et al. NCCN task force report: Update on the management of patients with gastrointestinal stromal tumors. J Natl Compr Canc Netw 2010;8 Suppl 2:S1-41.

- Yang CW, Liu XJ, Wei Y, Wan S, Ye Z, Yao S, et al. Use of computed tomography for distinguishing heterotopic pancreas from gastrointestinal stromal tumor and leiomyoma. Abdom Radiol (NY) 2021;46:168-78.
- Pinaikul S, Woodtichartpreecha P, Kanngurn S, Leelakiatpaiboon S. 1189 Gastrointestinal Stromal Tumor (GIST): Computed tomographic features and correlation of CT findings with histologic grade. J Med Assoc Thai 2014;97:1189-98.
- Vernuccio F, Taibbi A, Picone D, LA Grutta L, Midiri M, Lagalla R, et al. Imaging of gastrointestinal stromal tumors: From diagnosis to evaluation of therapeutic response. Anticancer Res 2016;36:2639-48.
- Xu J, Zhou J, Wang X, Fan S, Huang X, Xie X, et al. A multi-class scoring system based on CT features for preoperative prediction in gastric gastrointestinal stromal tumors. Am J Cancer Res 2020;10:3867-81.
- Cai PQ, Lv XF, Tian L, Luo ZP, Mitteer RA Jr., Fan Y, et al. CT characterization of duodenal gastrointestinal stromal tumors. AJR Am J Roentgenol 2015;204:988-93.